JACS
JOURNAL OF THE AMERICAN CHEMICAL SOCIETY
Article
pubs.acs.org/JACS

Molecular Dynamics of Dimethyldioxirane C−H Oxidation

Zhongyue Yang, Peiyuan Yu, and K. N. Houk*

Department of Chemistry and Biochemistry, University of California, Los Angeles, California 90095, United States

Supporting Information

ABSTRACT: We report molecular dynamics simulations of the reaction of dimethyldioxirane (DMDO) with isobutane. The reaction involves hydrogen atom abstraction in the transition state, and trajectories branch to the oxygen rebound pathway, which gives *tert*-butanol and acetone, or a separated radical pair. In the gas phase, only 10% of the reactive trajectories undergo the oxygen rebound pathway, but this increases to 90% in simulations in an implicit acetone solvent (SMD) because the oxygen rebound becomes barrierless in solution. Short-lived diradical species were observed in the oxygen rebound trajectories. The time gap between C−H bond-breaking and C−O bond formation ranges from 30 to 150 fs, close to the <200 fs lifetime of radical pairs from DMDO hydroxylation of *trans*-1-phenyl-2-ethylcyclopropane measured by Newcomb.

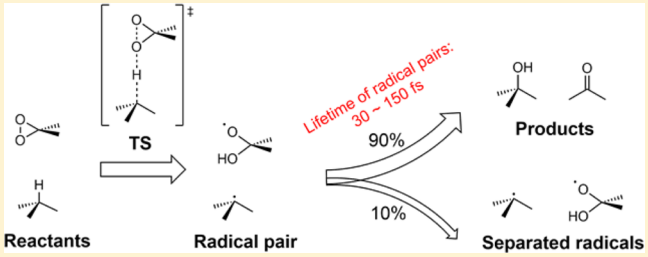

INTRODUCTION

Dioxiranes afford efficient and stereospecific oxyfunctionalizations of unactivated C−H bonds of alkanes under extremely mild conditions and without metal catalysts.[1−5] Three mechanisms have been proposed to rationalize the high efficiency and stereospecificity of dioxirane C−H oxidation. Murray and Curci suggested a concerted "oxenoid" mechanism (shown in Scheme 1a) based on kinetics, H/D isotope effects, selectivity, and stereochemical evidence.[2,5−8] This mechanism was challenged by Minisci, who showed that free radicals (shown in Scheme 1b) are involved in the reactions by trapping with $BrCCl_3$ or by conducting the experiment under an argon atmosphere.[9−11] Others argued against the free radical mechanism, citing stereospecific and stereoselective hydroxylations of *cis*- and *trans*-1,2-dimethylcyclohexane,[2] the lack of ring opening in hydroxylation of isopropylcyclopropane,[10] and ultrafast radical clock experiments.[12,13] This evidence, however, does not directly prove whether hydroxylation occurs by an oxenoid insertion reaction or by singlet radical pair formation and subsequent collapse (H-abstraction-O-rebound mechanism shown in Scheme 1c).

Scheme 1. Possible Mechanisms of Hydroxylation of Alkanes by Dioxiranes

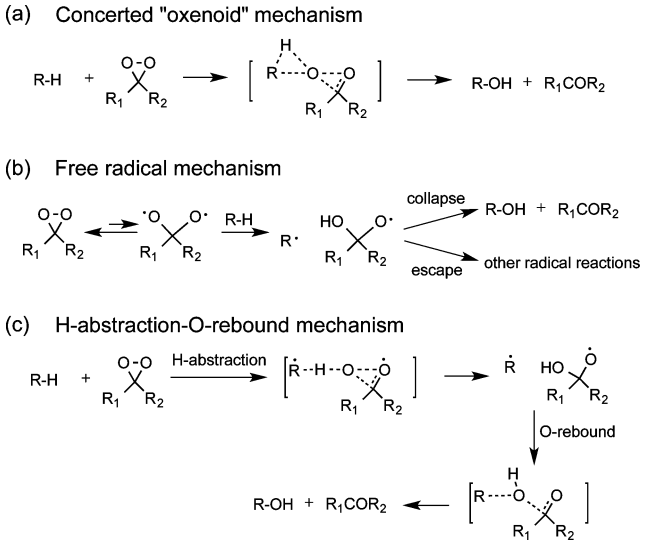

Bach, Fokin, Schreiner, Cremer, Sarzi-Amade, and Houk have all studied computationally a prototype of dimethyldioxirane (DMDO) C−H oxidations: the hydroxylation of isobutane.[14−21] The H-abstraction-O-rebound mechanism (Scheme 1c) was shown to be most favorable with an open-shell singlet TS in the rate-determining step (i.e., C−H abstraction). The diradical character of the TS originates from homolytic O−O bond cleavage of DMDO. It is noteworthy that in 1978, Goddard insightfully suggested that the dioxyl diradical form, dioxymethane (OCH_2O), could make a contribution to the chemistry of the parent dioxirane.[22]

As shown in Figure 1,[20] C−H abstraction results in a radical pair, which leads to the hydroxyl product through a no-barrier O-rebound transition state. Bach proposed a 7.3 kcal/mol barrier based on G4 calculations.[21] After the C−H abstraction, oxygen rebound has to be rapid enough to prevent radical pair diffusion; otherwise, stereoretention would be unlikely. Therefore, the time scale of oxygen rebound, or the lifetime of radical pair, is key to understanding the mechanism of DMDO hydroxylation.

Received: January 29, 2016
Published: March 10, 2016

DOI: 10.1021/jacs.6b01028
J. Am. Chem. Soc. 2016, 138, 4237−4242

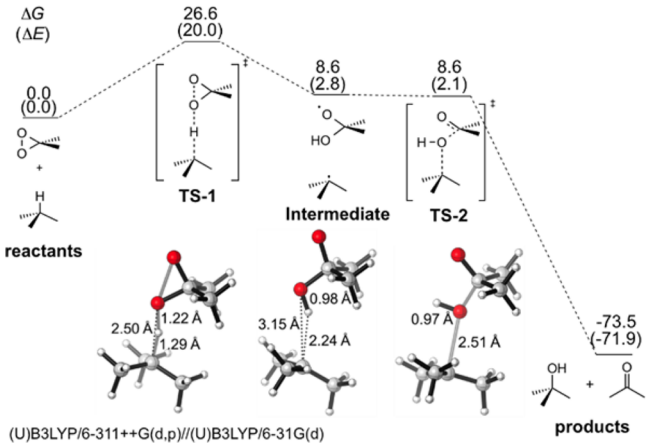

Figure 1. Free energy diagram of isobutane oxidation by DMDO in the gas phase.[20] Energies reported are in kcal mol^{-1}.

Newcomb conducted the DMDO hydroxylation of *trans*-1-phenyl-2-ethyl-cyclopropane to estimate the lifetime of radical pair. This ultrafast radical clock experiment, illustrated in Scheme 2, is based on the fact that C−H abstraction would give

Scheme 2. Ultrafast Radical Clock Experiment

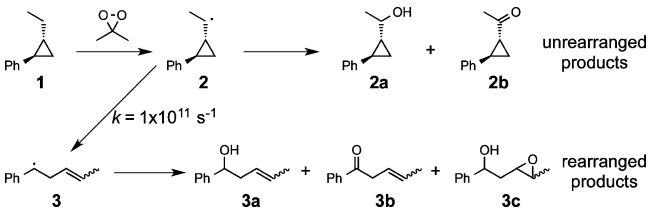

a radical known to rearrange with a rate constant of 10^{11} s^{-1}. The experiment gave very small amount of products identified as **3a−c**, giving a ratio of unrearranged to rearranged products of at least 40 at ambient temperature. This indicates that the rate constant for radical collapse is at least 4×10^{12} s^{-1}. Thus, it was proposed that the maximum lifetime of a putative radical pair is 200 fs,[12] a time scale only 3−4 times longer than that of a transition state (~60 fs).[23a−d]

Free radicals were clearly excluded by radical clock experiment, but whether and how short-lived radical pairs are involved in the DMDO oxidation remains unknown. Many assumptions were proposed for the oxygen rebound process. On one hand, solvent-caging effects,[24−28] consisting of steric hindrance and dipole stabilization, were generally assumed to facilitate rapid oxygen rebound. Steric hindrance could effectively inhibit radical pair dissociation, and solvent polarity might stabilize the dynamical species during the transformation from a moderately polar radical pair to very polar products (*tert*-butyl alcohol and acetone). On the other hand, non-statistical effects might be involved in the reaction, making the nascent radical pair carry dynamical memory, thus resulting in the products with stereoretention.[29−35] To explore how solvent effects and dynamics effects influence the oxygen rebound, we performed direct molecular dynamics (MD) simulations[36−39] on the DMDO C−H oxidation of isobutane in the gas phase and in implicit acetone. The solvent effect discussed here is only limited to solvent polarization because of the lack of explicit solvent molecules in implicit model.

COMPUTATIONAL METHODS

MD simulations were performed both in the gas phase and in implicit acetone solvent. For the gas phase MD studies, the open-shell singlet transition state (**TS-1** shown in Figure 1) for the reaction was located by QM method in Gaussian 09.[40] UB3LYP/6-31G(d) with HOMO−LUMO mixing for the initial guess was used in both transition state optimization and dynamics simulation. (U)B3LYP/6-311++G(d,p) single point energies were computed on the (U)B3LYP/6-31G(d)-optimized structures. We have previously shown that this method gives similar energetics compared to the multiconfigurational second-order perturbation method CASPT2 for this reaction.[20] The Cramer-Truhlar SMD solvation model was used for the implicit solvent calculations.[41] Quasiclassical direct-dynamics simulations were then initialized within the region of the potential energy surface near **TS-1**, adding zero-point energy for each real normal mode in **TS-1**, plus a Boltzmann sampling of thermal energy available at 300 K with a random phase. (The distribution of sampled transition state geometries is shown with overlay in Figure S1.) The trajectories were propagated forward and backward until the emergence of the final products (*tert*-butanol and acetone) (O_D−H_B < 1.15 Å and O_D−C_B < 1.59 Å, where D stands for DMDO and B stands for isobutane), radical pairs (O_D−H_B bond < 1.15 Å and O_D−C_B bond > 3.00 Å), or separated reactants (O_D−H_B bond > 5.00 Å). The classical equations of motion were integrated with a velocity-Verlet algorithm using Singleton's program Progdyn,[42] with the energies and derivatives computed on the fly by the UB3LYP method using Gaussian 09. The step length for integration was 1 fs. The MD simulations in implicit solvent followed the same protocol as the gas-phase MD studies, except that the location of the reaction saddle point and the propagation of trajectories were carried out in conjunction with a continuum solvation model.

RESULTS AND DISCUSSION

The free energy profile of DMDO C−H oxidation of isobutane with implicit acetone solvation (shown in Figure 2) was

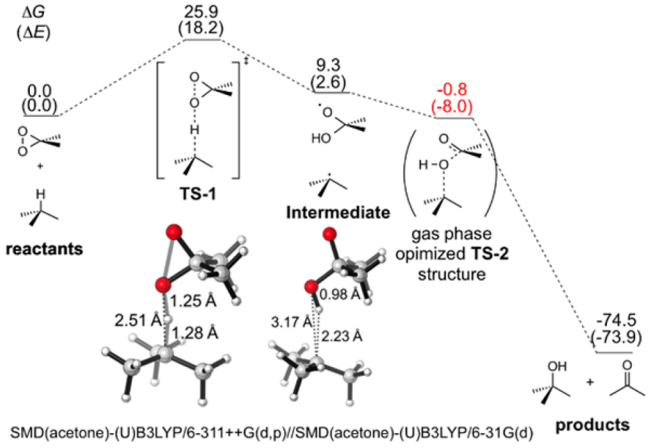

Figure 2. Free energy diagram of isobutane oxidation by DMDO in implicit solvent (acetone). Electronic energies are given in parentheses. **TS-2** cannot be located with solvation so that the energy reported in red is a single point based on the gas phase **TS-2** geometry. All energies reported are in kcal mol^{-1}.

obtained to compare to that in the gas phase (Figure 1). Implicit solvation has only a minor effect on the barrier of reaction ($\Delta\Delta G^{\ddagger}$ = 0.6 kcal/mol) and does not change the geometries of **TS-1** and **Intermediate** significantly. The oxygen-rebound transition state **TS-2** found in the gas phase (Figure 1) cannot be located with solvation. Unrestricted single-point calculations with implicit solvent on the gas phase optimized **TS-2** geometry result in a substantially lower energy than that of **Intermediate** (~10 kcal/mol). In addition, its

DOI: 10.1021/jacs.6b01028
J. Am. Chem. Soc. 2016, 138, 4237−4242

stable wave function shows no diradical character ($\langle S^2 \rangle = 0$). The estimated ~10 kcal/mol energy difference likely reflects an overestimate of the solvent stabilization, but the solvent effect is likely to be quite large. These results indicate that the oxygen rebound is barrierless in implicit acetone solvent. This originates from a crossover from singlet diradical character to zwitterionic character, which is better stabilized by polar solvation. (Shown in Figure S2.)

Figure 3 shows snapshots of two typical reactive trajectories for the hydroxylation of isobutane by DMDO in implicit acetone. Figure 3a is an oxygen-rebound trajectory, and Figure 3b is one in which the radical pair separates. The bond lengths of the O_D-H_B and O_D-C_B bonds are labeled on the graph, where the subscript D stands for DMDO and B stands for isobutane. Both trajectories involve similar transition states with H transfer from C to O, and O−O bond breaking. At 0 fs, the starting point for the trajectories in both directions, the forming O_D-H_B bond length is 0.98 Å for the oxygen-rebound trajectory, and 1.10 Å for the radical pair separation trajectory. The O_D-C_B bond length for the oxygen-rebound trajectory is 2.50 Å at 0 fs, 2.45 Å at 31 fs, and 1.58 Å at 80 fs. This shows that the oxygen on DMDO rebounds immediately after C−H abstraction and gives the final products, *tert*-butanol and acetone. We have defined "dynamically concerted" as reactions in which formation of two bonds in less than 60 fs, the time it takes to pass through a transition state.[23a−d] In the radical pair separation trajectory, the O_D-C_B bond length increases from 2.51 Å at 0 fs, to 2.61 Å at 35 fs, and to 3.55 Å at 200 fs; there is clear separation of the radicals.[43]

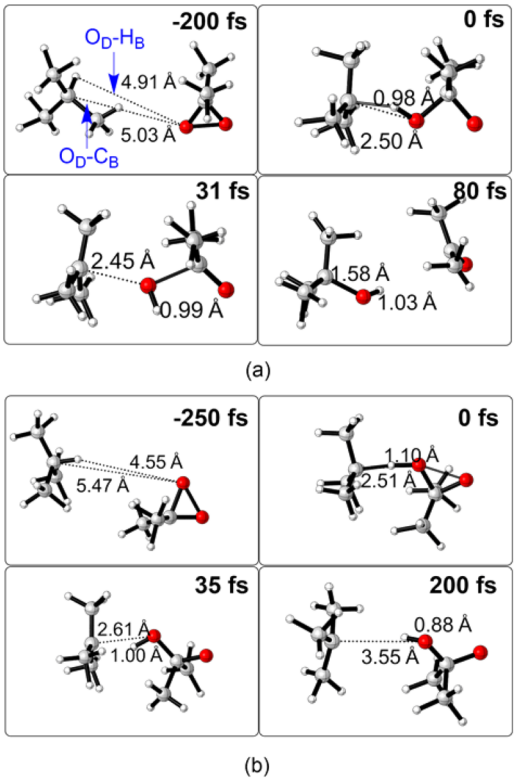

Figure 3. Snapshots of two typical reactive trajectories for the hydroxylation of isobutane by DMDO in implicit acetone. (a) An oxygen-rebound trajectory, in which DMDO hydroxylation of isobutane gives *tert*-butanol and acetone through oxygen rebound mechanism. (b) A radical pair separation pathway, in which *tert*-butyl and 2-oxidanylpropan-2-ol separate after C−H abstraction. The 0 fs panels correspond to the transition state geometry where trajectories are initiated.

Results for DMDO C−H oxidation of isobutane trajectories are summarized in Figure 4.[44] Figure 4a shows typical oxygen-rebound and radical pair separation trajectory represented by the O_D-H_B and O_D-C_B bond lengths. In the gas phase, 10% of the reactive trajectories directly lead to the alcohol (Figure 4b), while in implicit acetone solvent, the percentage increases to 90% (Figure 4c). Since oxygen rebound is barrierless in implicit acetone solvation, trajectories tend to propagate downhill to give the final product subsequent to the generation of the radical pair **Intermediate**. In contrast, gas-phase trajectories propagate on a relatively flat potential energy surface. They will give final product only after crossing the **TS-2**. Or even more likely, radical pair may drift apart during the propagation. Noticeably, spin contamination is significant when the radical pair separates. This might be another reason for the high proportion of radical-separation trajectories observed in the gas phase. Even so, the oxygen rebound trajectory observed in the gas phase does indicate a very rapid rebound, much faster than the rotational motion of the alkyl radical that would be needed to erode stereoselectivity.

Figure 4d displays the distribution of time gaps between the formation of O_D-H_B and O_D-C_B bonds in the oxygen-rebound trajectories propagated in implicit acetone solvent. We have previously defined two terms, "*dynamically concerted*" (time gap of formation of two bonds $\tau \leq 60$ fs) and "*dynamically stepwise*" (time gap of formation of two bonds $\tau > 60$ fs), to describe reaction mechanisms in a time-resolved fashion. Unlike the traditional concept of "*concerted*" and "*stepwise*", which focus on the existence of an intermediate on the PES, the new definitions are concerned about the involvement of fleeting intermediates in reactions based on dynamics.[45−47,23] The oxygen-rebound process is dynamically concerted ($\tau \leq 60$ fs) and stepwise ($\tau > 60$ fs). Only 35% of the time gaps are shorter than 60 fs, and 65% are longer than 60 fs. This duality of mechanism is exemplified in Figure 4e,f. Figure 4e shows a 45 fs-time-gap trajectory in which, subsequent to the formation of O_D-H_B bond, O_D-C_B bond oscillates around 2.5 Å for about one vibrational period of O_D-H_B bond and then decreases to 1.6 Å. This dynamical behavior indicates that no well-defined radical pair intermediate is generated along the trajectory, suggesting a dynamically concerted mechanism. Figure 4f displays a 115 fs-time-gap trajectory where, subsequent to the formation of O_D-H_B bond, the O_D-C_B bond increases to about 3.0 Å and undergoes several vibrational motions of the O_D-H_B bond before the formation of O_D-C_B bond. This trajectory involves a fleeting radical pair, which geometrically resembles the **Intermediate** shown in Figure 2, suggestive of a dynamically stepwise mechanism.

The implicit acetone model provides qualitative understanding of how solvent polarity influences oxygen rebound. However, the model has some limitations. The model intrinsically treats dynamical species using a fully adiabatically optimized equilibrium continuum surrounding. In reality, however, solvent reorientation and relaxation may take several picoseconds or even longer.[48−52] On the time scale of oxygen rebound, the solvent will be approximately stationary, which is inconsistent with the adabatic behavior assumed by implicit solvation. In addition, the implicit solvation does not account for the steric hindrance with solvent cage. These facts highlight

DOI: 10.1021/jacs.6b01028
J. Am. Chem. Soc. 2016, 138, 4237−4242

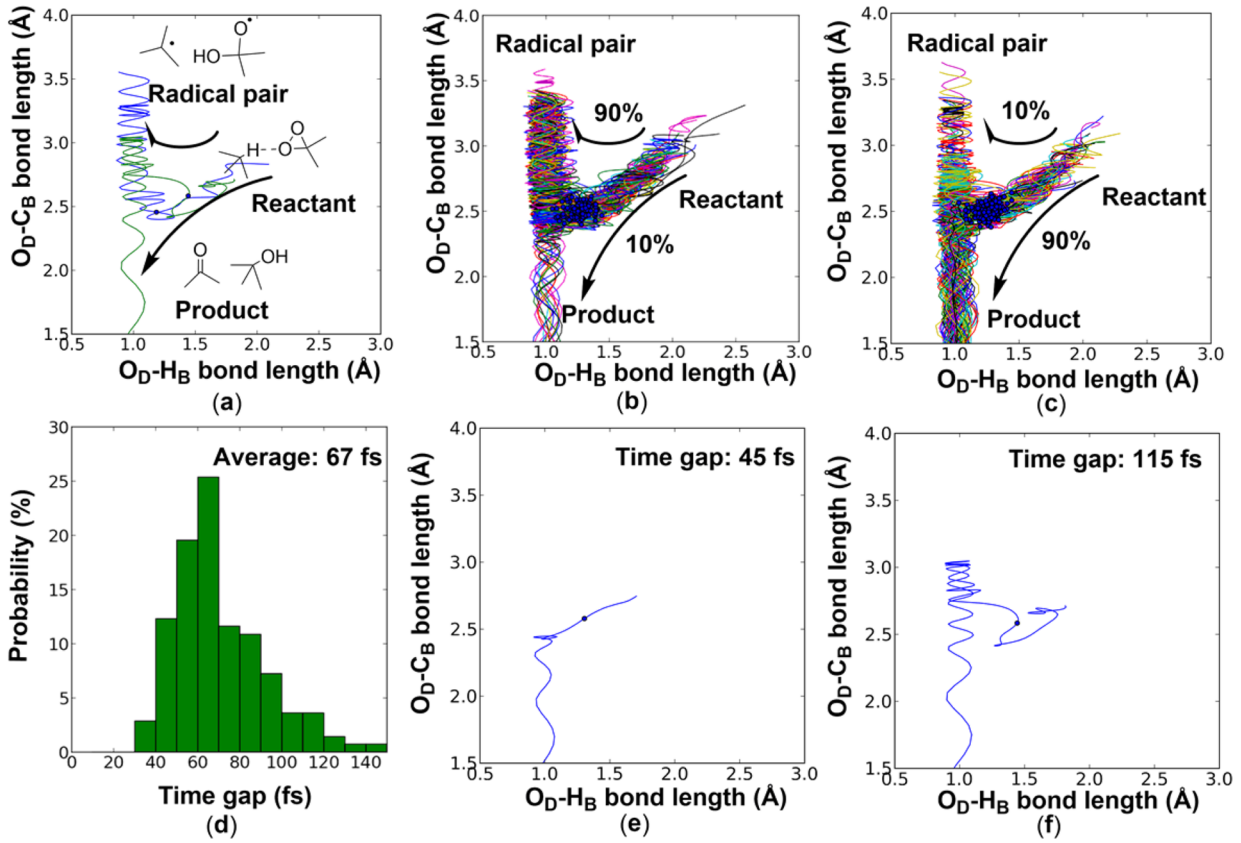

Figure 4. (a) A typical oxygen-rebound and recrossing trajectory represented by the O_D-H_B and O_D-C_B bond lengths. The labels are consistent with Figure 3. (b) Distribution of 100 reactive trajectories propagated in the gas phase. (c) Distribution of 100 reactive trajectories propagated in implicit acetone. (d) Distribution of time gap between formation of the O_D-H_B and O_D-C_B bond. The time gap is extracted from the oxygen-rebound trajectories propagated in implicit acetone solvent. The criteria for O_D-H_B and O_D-C_B bond formation are set as 1.2 and 1.6 Å, respectively. (e) An oxygen-rebound trajectory with 45 fs time gap. (f) An oxygen-rebound trajectory with 115 fs time gap. Blues dots labeled in (a–c), (e), and (f) are sampled transition state used to initiate trajectories.

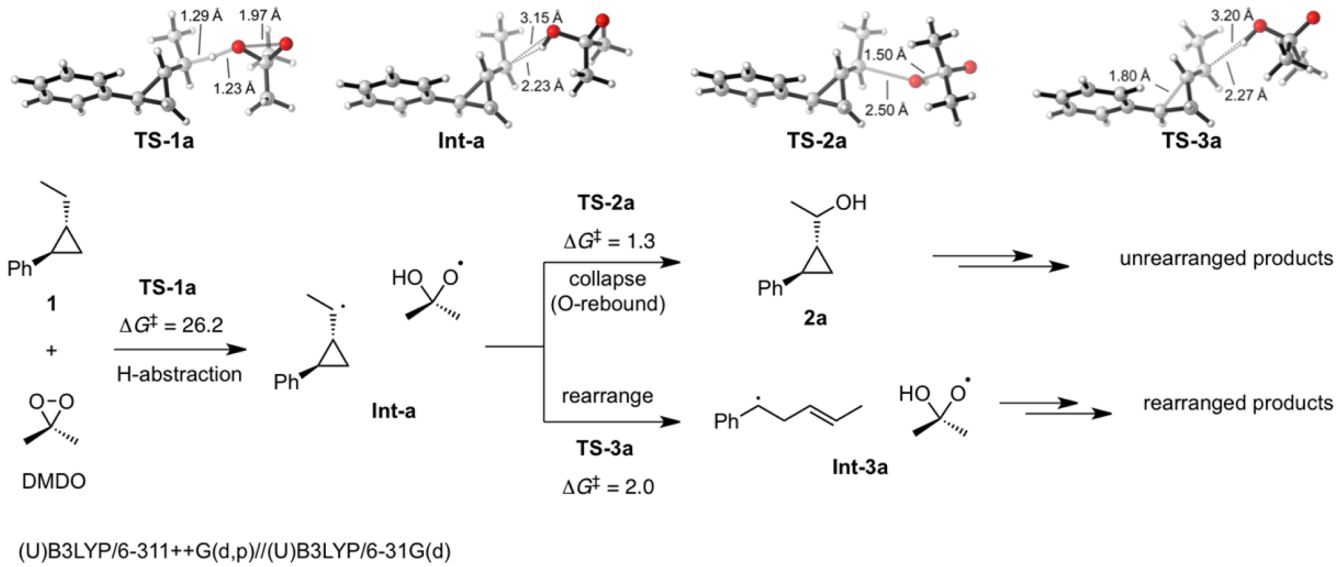

Figure 5. Computed gas phase energetics of DMDO hydroxylation of *trans*-1-phenyl-2-ethylcyclopropane (Newcomb's radical clock experiment). Energies reported are in kcal mol^{-1}.

the necessity of dynamics simulations with explicit solvent, which is ongoing work in our group.

In Newcomb's radical clock experiment (Scheme 2), the substrate (**1**) generates the more complex secondary radical. We have computed the energetics of the reaction with DMDO. The results are shown in Figure 5. In the gas phase, the H-abstraction step has a free energy of activation of 26.2 kcal/mol, very close to that of isobutane oxidation (Figure 1, 26.6 kcal/

DOI: 10.1021/jacs.6b01028
J. Am. Chem. Soc. 2016, 138, 4237–4242

mol). Once the radical pair forms, it may collapse (O-rebound) to form alcohol **2a**, or rearrange to form radical pair **Int-3a** (as well as its *cis* isomer, not shown).

The O-rebound has a barrier of 1.3 kcal/mol in the gas phase, but the barrier disappears with implicit acetone solvent, similar to the isobutane case. The radical rearrangement has a barrier of 2.0 kcal/mol, in good agreement with the rate constant measured by Newcomb (10^{11} s^{-1}) based on transition state theory. The experimental ratio of unrearranged to rearranged products is greater than 40:1,[12] which indicates that the energy barrier of O-rebound is 2.2 kcal/mol lower than that of rearrangement at ambient temperature. This further supports that the O-rebound step has no barrier in solvent. The lifetimes of radical pairs computed for the isobutane case are shown in Figure 4d; the time spans of radical pairs involved in DMDO C−H oxidation of isobutane are between 30 and 150 fs. These are consistent with the lifetime of radical pairs measured by Newcomb from DMDO C−H oxidation of *trans*-1-phenyl-2-ethylcyclopropane (<200 fs).[12]

CONCLUSION

We have studied the molecular dynamics of DMDO C−H oxidation of isobutane. The free energy profile of the reaction was calculated, and indicates that the oxygen rebound is barrierless in acetone solvation. In MD simulations, oxygen-rebound and radical pair separation pathways were identified. The percentage of oxygen-rebound trajectories is 10% in the gas phase and 90% in implicit acetone solvent. This indicates that the solvent influences the oxygen rebound, by response to the polarity change during hydroxyl group transfer. Analysis of oxygen rebound trajectories indicates that both dynamically concerted and stepwise mechanisms are observed. The time gaps of oxygen rebound (i.e., the lifetime of radical pairs) from DMDO C−H oxidation of isobutane range from 30 to 150 fs. For comparison, Newcomb estimated the lifetime of the radical pair to be <200 fs in his radical clock experiment involving DMDO C−H oxidation of *trans*-1-phenyl-2-ethylcyclopropane.[12]

ASSOCIATED CONTENT

Supporting Information

. . The Supporting Information is available free of charge on the ACS Publications website at DOI: 10.1021/jacs.6b01028.

Movie of reactive trajectory shown in Figure 3a (MPG)
Movie of reactive trajectory shown in Figure 3b (MPG)
Input parameters for Progdyn; results for transition state normal model sampling in the gas phase and in acetone solvation; charge distribution analysis on **TS-2** shown in Figure 2; coordinates and energies of stationary points (PDF)

AUTHOR INFORMATION

Corresponding Author

*houk@chem.ucla.edu

Notes

The authors declare no competing financial interest.

ACKNOWLEDGMENTS

We are grateful to Prof. Daniel Singleton, Yu-hong Lam, Lufeng Zou, Yong Liang, Xin Hong, and Gonzalo Jiménez-Osés for helpful discussions. This work was supported by the National Science Foundation (CHE-1361104), and NSF under the CCI Center for Stereoselective C−H Functionalization (CHE-1205646). Calculations were performed on the Hoffman2 cluster at UCLA and the Extreme Science and Engineering Discovery Environment (XSEDE), which is supported by the National Science Foundation.

REFERENCES

(1) Murray, R. W.; Jeyaraman, R. *J. Org. Chem.* **1985**, *50*, 2847.
(2) Murray, R. W.; Jeyaraman, R.; Mohan, L. *J. Am. Chem. Soc.* **1986**, *108*, 2470.
(3) Adam, W.; Curci, R.; Edwards, J. O. *Acc. Chem. Res.* **1989**, *22*, 205.
(4) (a) Chen, K.; Eschenmoser, A.; Baran, P. S. *Angew. Chem., Int. Ed.* **2009**, *48*, 9705. (b) Chen, K.; Baran, P. S. *Nature* **2009**, *459*, 824. (c) Gaich, T.; Baran, P. S. *J. Org. Chem.* **2010**, *75*, 4657. (d) Michaudel, Q.; Journot, G.; Regueiro-Ren, A.; Goswami, A.; Guo, Z.; Tully, T. P.; Zou, L.; Ramabhadran, R. O.; Houk, K. N.; Baran, P. S. *Angew. Chem., Int. Ed.* **2014**, *53*, 12091.
(5) Curci, R.; Dinoi, A.; Rubino, M. F. *Pure Appl. Chem.* **1995**, *67*, 811.
(6) Mello, R.; Fiorentino, M.; Fusco, C.; Curci, R. *J. Am. Chem. Soc.* **1989**, *111*, 6749.
(7) Adam, W.; Asensio, G.; Curci, R.; Gonzaleznunez, M. E.; Mello, R. *J. Org. Chem.* **1992**, *57*, 953.
(8) Murray, R. W.; Singh, M.; Jeyaraman, R. *J. Am. Chem. Soc.* **1992**, *114*, 1346.
(9) Minisci, F.; Zhao, L.; Fontana, F.; Bravo, A. *Tetrahedron Lett.* **1995**, *36*, 1697.
(10) Vanni, R.; Garden, S. J.; Banks, J. T.; Ingold, K. U. *Tetrahedron Lett.* **1995**, *36*, 7999.
(11) Bravo, A.; Bjorsvik, H.-R.; Fontana, F.; Minisci, F.; Serri, A. *J. Org. Chem.* **1996**, *61*, 9409.
(12) Simakov, P. A.; Choi, S.-Y.; Newcomb, M. *Tetrahedron Lett.* **1998**, *39*, 8187.
(13) Curci, R.; D'Accolti, L.; Fusco, C. *Tetrahedron Lett.* **2001**, *42*, 7087.
(14) Cremer, D.; Kraka, E.; Szalay, P. G. *Chem. Phys. Lett.* **1998**, *292*, 97.
(15) Shustov, G. V.; Rauk, A. *J. Org. Chem.* **1998**, *63*, 5413.
(16) Bach, R. D.; Andres, J. L.; Su, M. D.; McDouall, J. J. W. *J. Am. Chem. Soc.* **1993**, *115*, 5768.
(17) Bach, R. D.; Su, M. D. *J. Am. Chem. Soc.* **1994**, *116*, 10103.
(18) Fokin, A. A.; Tkachenko, B. A.; Korshunov, O. I.; Gunchenko, P. A.; Schreiner, P. R. *J. Am. Chem. Soc.* **2001**, *123*, 11248.
(19) Freccero, M.; Gandolfi, R.; Sarzi-Amade, M.; Rastelli, A. *J. Org. Chem.* **2003**, *68*, 811.
(20) Zou, L.; Paton, R. S.; Eschenmoser, A.; Newhouse, T. R.; Baran, P. S.; Houk, K. N. *J. Org. Chem.* **2013**, *78*, 4037.
(21) Bach, R. D. *J. Phys. Chem. A* **2016**, *120*, 840.
(22) Harding, L. B.; Goddard, W. A. *J. Am. Chem. Soc.* **1978**, *100*, 7180.
(23) (a) Black, K.; Liu, P.; Xu, L.; Doubleday, C.; Houk, K. N. *Proc. Natl. Acad. Sci. U. S. A.* **2012**, *109*, 12860. (b) Xu, L.; Doubleday, C. E.; Houk, K. N. *Angew. Chem., Int. Ed.* **2009**, *48*, 2746. (c) Xu, L.; Doubleday, C. E.; Houk, K. N. *J. Am. Chem. Soc.* **2010**, *132*, 3029. (d) Xu, L.; Doubleday, C. E.; Houk, K. N. *J. Am. Chem. Soc.* **2011**, *133*, 17848.
(24) Yang, H.; Snee, P. T.; Kotz, K. T.; Payne, C. K.; Harris, C. B. *J. Am. Chem. Soc.* **2001**, *123*, 4204.
(25) Koneshan, S.; Rasaiah, J. C.; Lynden-Bell, R. M.; Lee, S. H. *J. Phys. Chem. B* **1998**, *102*, 4193.
(26) Wan, C.; Gupta, M.; Baskin, J. S.; Kim, Z. H.; Zewail, A. H. *J. Chem. Phys.* **1997**, *106*, 4353.
(27) Liu, Q.; Wang, J.-K.; Zewail, A. H. *Nature* **1993**, *364*, 427.
(28) Van Der Zwan, G.; Hynes, J. T. *Chem. Phys. Lett.* **1983**, *101*, 367.
(29) Bogle, X. S.; Singleton, D. A. *Org. Lett.* **2012**, *14*, 2528.
(30) Oyola, Y.; Singleton, D. A. *J. Am. Chem. Soc.* **2009**, *131*, 3130.

DOI: 10.1021/jacs.6b01028
J. Am. Chem. Soc. 2016, 138, 4237−4242

(31) Collins, P.; Kramer, Z. C.; Carpenter, B. K.; Ezra, G. S.; Wiggins, S. *J. Chem. Phys.* **2014**, *141*, 034111.
(32) Carpenter, B. K. *Chem. Rev.* **2013**, *113*, 7265.
(33) Litovitz, A. E.; Keresztes, I.; Carpenter, B. K. *J. Am. Chem. Soc.* **2008**, *130*, 12085.
(34) Glowacki, D. R.; Marsden, S. P.; Pilling, M. J. *J. Am. Chem. Soc.* **2009**, *131*, 13896.
(35) Glowacki, D. R.; Liang, C. H.; Marsden, S. P.; Harvey, J. N.; Pilling, M. J. *J. Am. Chem. Soc.* **2010**, *132*, 13621.
(36) Doubleday, C.; Suhrada, C. P.; Houk, K. N. *J. Am. Chem. Soc.* **2006**, *128*, 90.
(37) Suhrada, C. P.; Houk, K. N. *J. Am. Chem. Soc.* **2002**, *124*, 8796.
(38) Houk, K. N.; Nendel, M.; Wiest, O.; Storer, J. W. *J. Am. Chem. Soc.* **1997**, *119*, 10545.
(39) Carpenter, B. K. *J. Am. Chem. Soc.* **1995**, *117*, 6336.
(40) Frisch, M. J.; Trucks, G. W.; Schlegel, H. B.; Scuseria, G. E.; Robb, M. A.; Cheeseman, J. R.; Scalmani, G.; Barone, V.; Mennucci, B.; Petersson, G. A.; Nakatsuji, H.; Caricato, M.; Li, X.; Hratchian, H. P.; Izmaylov, A. F.; Bloino, J.; Zheng, G.; Sonnenberg, J. L.; Hada, M.; Ehara, M.; Toyota, K.; Fukuda, R.; Hasegawa, J.; Ishida, M.; Nakajima, T.; Honda, Y.; Kitao, O.; Nakai, H.; Vreven, T.; Montgomery Jr., J. A.; Peralta, J. E.; Ogliaro, F.; Bearpark, M. J.; Heyd, J.; Brothers, E. N.; Kudin, K. N.; Staroverov, V. N.; Kobayashi, R.; Normand, J.; Raghavachari, K.; Rendell, A. P.; Burant, J. C.; Iyengar, S. S.; Tomasi, J.; Cossi, M.; Rega, N.; Millam, N. J.; Klene, M.; Knox, J. E.; Cross, J. B.; Bakken, V.; Adamo, C.; Jaramillo, J.; Gomperts, R.; Stratmann, R. E.; Yazyev, O.; Austin, A. J.; Cammi, R.; Pomelli, C.; Ochterski, J. W.; Martin, R. L.; Morokuma, K.; Zakrzewski, V. G.; Voth, G. A.; Salvador, P.; Dannenberg, J. J.; Dapprich, S.; Daniels, A. D.; Farkas, Ö.; Foresman, J. B.; Ortiz, J. V.; Cioslowski, J.; Fox, D. J.; Gaussian, Inc.: Wallingford, CT,, 2009.
(41) Marenich, A. V.; Cramer, C. J.; Truhlar, D. G. *J. Phys. Chem. B* **2009**, *113*, 6378.
(42) Singleton, D. A.; Wang, Z. H. *J. Am. Chem. Soc.* **2005**, *127*, 6679.
(43) Propagation of the trajectory for even longer time (~500 fs) leads to the further separation of the radical pair.
(44) In Figure 4b,c, we show the distribution of the reactive trajectories, which are defined as trajectories starting from reactants and lead to rebound product or radical pair. In the dynamics simulations, we obtained reactive trajectories, recrossing trajectories, and product-to-radical pair trajectories. The percentage for there three types are around 60%, 35%, and 5%, respectively.
(45) Patel, A.; Chen, Z.; Yang, Z.; Gutierrez, O.; Liu, H.-w.; Houk, K. N.; Singleton, D. A. *J. Am. Chem. Soc.* **2016**, DOI: 10.1021/jacs.6b00017.
(46) Yang, Z.; Doubleday, C.; Houk, K. N. *J. Chem. Theory Comput.* **2015**, *11*, 5606.
(47) Hong, X.; Bercovici, D. A.; Yang, Z.; Al-Bataineh, N.; Srinivasan, R.; Dhakal, R. C.; Houk, K. N.; Brewer, M. *J. Am. Chem. Soc.* **2015**, *137*, 9100.
(48) Nandi, N.; Bhattacharyya, K.; Bagchi, B. *Chem. Rev.* **2000**, *100*, 2013.
(49) Bagchi, B.; Biswas, R. *Adv. Chem. Phys.* **1999**, *109*, 207.
(50) Hamm, P.; Lim, M.; Hochstrasser, R. M. *J. Chem. Phys.* **1997**, *107*, 10523.
(51) Voth, G. A.; Hochstrasser, R. M. *J. Phys. Chem.* **1996**, *100*, 13034.
(52) Chen, Z.; Nieves-Quinones, Y.; Waas, J. R.; Singleton, D. A. *J. Am. Chem. Soc.* **2014**, *136*, 13122.

DOI: 10.1021/jacs.6b01028
J. Am. Chem. Soc. 2016, 138, 4237−4242